Investigation of biochar production potential and pyrolysis kinetics characteristics of microalgal biomass

Anıl Tevfik Koçer [1] · Burak Mutlu [1] · Didem Özçimen [1]

Abstract

In the present work, the effect of pyrolysis conditions on biochar yield obtained from *Chlorella vulgaris* was examined statistically and the pyrolysis kinetics was determined using a thermogravimetric analyzer. For the production of biochar from microalgae, pyrolysis was carried out at the temperatures of 300, 500, and 700 °C, with the heating rates of 5, 15, and 25 °C/min, retention time of 0, 15, and 30 min, and nitrogen flow rate of 100 ml/min. For the examination of pyrolysis kinetic parameters, dried microalga was heated up to 900 °C at four different heating values of 5, 10, 25, and 50 °C/min at a constant nitrogen flow rate of 40 ml/min. Optimum pyrolysis conditions and the most suitable pyrolysis kinetic model were determined for *Chlorella vulgaris*. According to the obtained results, it was seen that *Chlorella vulgaris* could be easily evaluated in thermal conversion processes. Also, these results provide valuable information for optimization of biochar production, and modeling and designing of new pyrolysis systems using microalgal biomass.

1 Introduction

Today, approximately 80% of the world's energy needs are met by fossil energy sources such as petroleum, natural gas, and coal. Although fossil fuels are the major energy sources in the world, they can lead to serious environmental problems such as global warming and air pollution, and they have limited reserves [1]. Due to these disadvantages of using fossil resources, researches on renewable energy sources such as sun, wind, hydraulics, and biomass are constantly increasing day by day [2, 3].

Biomass is considered as an important renewable energy source because it can be converted into different biofuels such as biogas, bioethanol, biodiesel, and biochar [4]. Biofuels can be classified as first, second, and third generation biofuels according to the feedstock type. First generation biofuels are generated from food crops; second generation biofuels are generated from non-food and lignocellulosic waste biomass; and third generation biofuels are generated from algal biomass [5]. There is a concern about food safety considering that conversion methodologies for biofuel production use agricultural food products which are first generation sources such as crops, corn, soybean, wheat, etc. So, researchers have focused on second generation biofuels to avoid consuming food stocks. However, the biofuel production from second generation sources such as lignocellulosic materials and wastes is not an economical way yet, because of their hard degradation. It is both more costly and more complex. Therefore, the researchers focused on third generation biofuels [6]. Unlike the first and second generation biofuel feedstocks, algal biomass including macro and microalgae can be cultivated easily, efficiently, and economically [7]. And third generation sources such as macroalgae, microalgae, and other aquatic plants are so useful to produce third generation biofuels without food safety debate. These sources will not threaten food security in any way. So, their utilization is a very important way for biofuel production.

In recent years, many important studies have been carried out on biofuel production from algae. Nautiyal et al. [8] studied biodiesel production from *Chlorella pyrenoidosa* and *Spirulina platensis* because of the high lipid content of these microalgae species and they found that the microalgal biodiesel can be comparable with the conventional biodiesel.

✉ Didem Özçimen
ozcimen@yildiz.edu.tr

1 Faculty of Chemical and Metallurgical Engineering, Bioengineering Department, Yıldız Technical University, Esenler, 34220 Istanbul, Turkey

Bohutskyi et al. [9] also produced biogas under mesophilic conditions by using lipid extracted *Chlorella protothecoides* via anaerobic digestion. They notified that algal biomass can be used for biogas production via anaerobic digestion/co-digestion. Reyimu and Özçimen [10] obtained bioethanol from alkaline pretreated *Nannochloropsis oculata* and *Tetraselmis suecica* via fermentation. Chaiwong et al. [11] produced biochar and bio-oil from *Spirulina* sp. via slow pyrolysis.

The pyrolysis process is one of the common thermochemical conversion methods to produce biofuels such as bio-oil and biochar at high temperatures in the inert atmosphere [12]. Pyrolysis products (biochar and bio-oil) can be used in different areas such as energy, environment, and agriculture. For instance, bio-oil can be used for the production of valuable biochemicals and fuels while biochar can be used for heat generation, adsorption, and soil improvement [13]. In the literature, biochar production from algae, pyrolysis characteristics, and kinetics of algal biomass have been studied by many researchers. Bird et al. [14] selected eight species of green tide filamentous macroalgae for the biochar production and they obtained biochars at final temperatures of 307, 414, 450, and 512 °C. Yanik et al. [15] produced biochars from *Laminaria digitata* and *Fucus serratus* at a temperature of 500 °C. Miao et al. [16] studied the fast pyrolysis of *C. protothecoides* and *Microcystis aeruginosa* at a temperature of 500 °C. Also, Yang et al. [17], Radhakumari et al. [18], Plis et al. [19], and Agrawal and Chakraborty [20] have performed pyrolysis of different macro and microalgae species and they have determined the pyrolysis kinetics parameters in their studies.

In this study, biochar production from *Chlorella vulgaris*, cultivated in Yıldız Technical University, Algal Biotechnology Laboratory, was carried out and effects of pyrolysis conditions on biochar yields were investigated statistically using Box-Behnken factorial design. Box-Behnken factorial design, required three levels of each factor, is a useful method for developing and optimizing processes, and it is used to correlate the dependent and independent variables to develop the second-order response surface model [21, 22]. So, this design was applied to evaluate the effects of the three selected independent variables such as temperature, heating rate, and retention time on biochar yield in this study. Also, some characterization analyses were performed on the raw microalga and microalgal biochar. Moreover, pyrolysis kinetic parameters of microalga were determined using a thermogravimetric analyzer. Kinetic parameters are calculated using the Kissinger-Akahira-Sunose (KAS), Flynn–Wall–Ozawa (FWO), and Coats-Redfern (CR) methods. In the literature, there is no any studies which investigate biochar potential of *Chlorella vulgaris* microalgae statistically and by pyrolysis kinetics simultaneously in detail.

2 Materials and methods

2.1 Sample preparation and characterization

Chlorella vulgaris was selected for biochar production and determination of pyrolysis kinetics. This microalga strain was obtained from the Culture Collection of Algae at Göttingen University (Goettingen, Germany) and it was grown in BG-11 medium, which was prepared according to literature Koçer and Özçimen [23]. Cultivation of *Chlorella vulgaris* was performed in a photobioreactor (5 l) under continuous white fluorescent light illumination (8000 lx) and at room temperature for 15 days. Then, the microalgae were centrifuged for 15 min at 5000 rpm, dried at the temperature of 60 °C for a night, and stored.

For characterization of microalgae samples, biochemical content and functional groups were determined and proximate analysis was performed. The functional groups of microalga were determined by Bruker Alpha FTIR equipment. The carbohydrate, lipid, and protein contents of *C. vulgaris* were determined by the phenol-sulfuric acid method [24], the Soxhlet extraction method [25], and the Lowry method [26], respectively. The phenol-sulfuric acid method and Lowry method were performed according to Dubois et al. [24] and Lowry et al. [26] using glucose and BSA as standards, respectively. The Soxhlet extraction was also carried out according to Soxhlet [25] using hexane as a solvent. For determination of carbohydrate and protein contents, PG Instruments T60 UV-visible spectrophotometer was used. All chemicals used in these methods were obtained from Merck Millipore (Darmstadt, Germany). The proximate analysis was performed using TA Instruments SDT Q600 thermogravimetric analyzer, and the moisture, volatile matter, fixed carbon, and ash contents of *C. vulgaris* were determined according to ASTM protocols [27].

2.2 Carbonization process

In the experiments, a split furnace (Protherm, ASP 11/100/500) was used for the carbonization process and the effects of temperature, heating rate, and residence time on the biochar yields were investigated. The split furnace is in dimensions of 51 cm × 40 cm × 50 cm, and the diameter of the pipe reactor in the furnace is 10 cm. The temperature control is provided by the Honeywell DC1010 PID controller. Experimental conditions were selected as temperatures of 300, 500, and 700 °C, heating rates of 5, 15, and 25 °C/min, retention times of 0, 15, and 30 min, and nitrogen flow rate of 100 ml/min. A 10-g sample of dried *C. vulgaris* was placed in the split furnace in porcelain vessels having high temperature resistance. Before the system is switched to heating, it is purged with nitrogen gas for 15 min to provide an inert environment. At the end of the carbonization process, biochars were taken from the

Table 1 Box-Behnken design matrix and experimental results

Run	Operating conditions			Coded factors			Biochar yield (%)
	Temperature (°C)	Heating rate (°C/min)	Retention time (min)	X_1	X_2	X_3	
1	700	15	30	1	0	1	18.41
2	500	25	0	0	1	−1	26.56
3	500	25	30	0	1	1	24.44
4	700	15	0	1	0	−1	18.74
5	300	5	15	−1	−1	0	41.13
6	500	15	15	0	0	0	20.63
7	500	15	15	0	0	0	20.66
8	500	5	30	0	−1	1	19.04
9	500	5	0	0	−1	−1	26.56
10	700	25	15	1	1	0	23.64
11	500	15	15	0	0	0	20.45
12	300	25	15	−1	1	0	45.10
13	500	15	15	0	0	0	20.65
14	300	15	30	−1	0	1	36.54
15	700	5	15	1	−1	0	19.56
16	500	15	15	0	0	0	20.58
17	300	15	5	−1	0	−1	53.61

furnace and then weighed to calculate the solid product yield [28].

2.3 Experimental design

Design Expert 7 statistical software package was used for experimental design to evaluate the relationship between solid product yield and process parameters such as temperature, heating rate, and retention time. The Box-Behnken design matrix was shown in Table 1 and temperature, heating rate, and retention time parameters were defined as X_1, X_2, and X_3, respectively. Solid product yield as the response of equation was defined with Y. Each parameter was coded at three levels: − 1 (minimum), 0 (central), and + 1 (maximum).

2.4 Pyrolysis kinetics

The TA Instruments SDT Q600 thermogravimetric analyzer was used to determine the pyrolysis kinetics of microalga. Approximately 4 mg of *Chlorella vulgaris* was placed in an alumina crucible and heated up to 900 °C with four heating rates (5, 10, 25, 50 °C/min) in the inert atmosphere. The nitrogen gas was used as a sweep gas and nitrogen flow rate was maintained at 100 ml/min.

Table 2 Kinetic models and mathematical expressions

Kinetic models	Mechanism	$f(\alpha)$	$g(\alpha)$
Based on the diffusion mechanisms			
D_1	Plane symmetry	$1/2\alpha$	α^2
D_2	Cylindrical symmetry	$[-\ln(1-\alpha)]^{-1}$	$(1-\alpha)\ln(1-\alpha)+\alpha$
D_3	Three-dimensional	$(3/2)(1-\alpha)^{2/3}[1-(1-\alpha)^{1/3}]^{-1}$	$[1-(1-\alpha)^{1/3}]^2$
D_4	Spherical symmetry	$(3/2)[(1-\alpha)^{-1/3}-1]^{-1}$	$(1-2\alpha/3)-(1-\alpha)^{2/3}$
Based on geometrical models			
R_1	Plane symmetry	1	α
R_2	Cylindrical symmetry	$2(1-\alpha)^{1/2}$	$1-(1-\alpha)^{1/2}$
R_3	Spherical symmetry	$3(1-\alpha)^{2/3}$	$1-(1-\alpha)^{1/3}$
Based on the order of reaction			
F_1	First order	$1-\alpha$	$-\ln(1-\alpha)$
F_2	Second order	$(1-\alpha)^2$	$-1+(1-\alpha)^{-1}$
F_3	Third order	$(1-\alpha)^3$	$[-1+(1-\alpha)^{-2}]/2$

Table 3 Biochemical and proximate analysis of *Chlorella vulgaris*

Parameters	*Chlorella vulgaris*
Protein (%)	33.64
Carbohydrates (%)	25.30
Lipids (%)	19.61
Moisture (%)	6.78
Volatile matter (%)	82.20
Fixed carbon (%)	6.12
Ash (%)	4.90

For the determination of kinetic parameters such as the activation energy and pre-exponential factor, the methods are based on the following three equations [29]:

$$T = T_0 + \beta . t \tag{1}$$
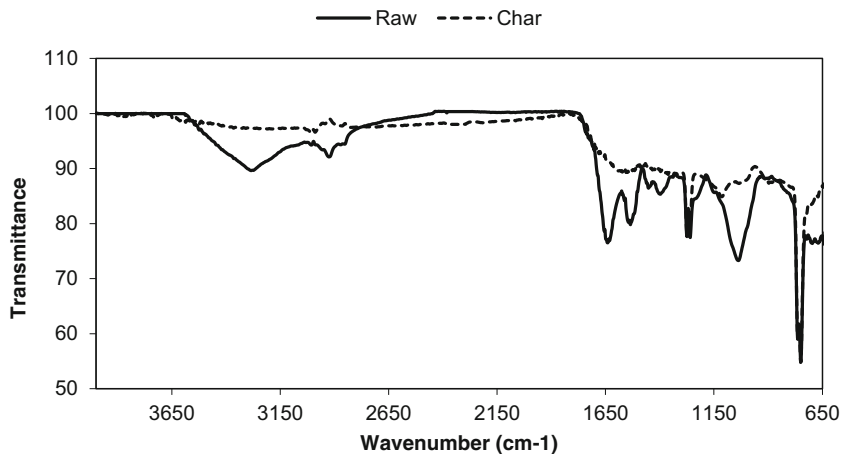
$$\frac{d\alpha}{dt} = k . f(\alpha) \tag{2}$$

$$k = A . \exp\left(\frac{-E}{R.T}\right) \tag{3}$$

In Eq. (1), T, T_0, and β express the temperature at time t, the initial temperature, and the linear heating rate, respectively. In Eq. (2), k and α express the rate constant and the degree of conversion. In Eq. (3), A, E, and R values express the pre-exponential factor, activation energy, and the gas constant, respectively.

The degree of conversion (α) can be calculated by the following equation:

$$\alpha = \frac{W_0 - W_t}{W_0 - W_f} \tag{4}$$

where W_0 is the sample mass at the initial time, W_t is the sample mass at time t, and W_f is the sample mass at the end of the reaction. $f(\alpha)$ is a certain function of α, and there are various models, which are designated in Table 2 [30].

The combination of Eqs. (1)–(4) gives the following relationship:

- Kissinger-Akahira-Sunose (KAS) method [31] expressed as follows:

$$\ln\left[\frac{\beta}{T^2}\right] = \ln\left[\frac{A.R}{E.g(\alpha)}\right] - \frac{E}{R.T} \tag{5}$$

where the plot of $\ln(\beta/T^2)$ versus $1/T$ gives a straight line from which the slope was used to determine the activation energy.

- Flynn–Wall–Ozawa (FWO) method [32, 33] expressed as follows:

$$\ln\beta = \ln\left[\frac{A.E}{R.g(\alpha)}\right] - 5.331 - 1.052\frac{E}{R.T} \tag{6}$$

where the plot of $\ln(\beta)$ versus $1/T$ gives a straight line from which the slope was used to determine the activation energy.

- Coats-Redfern (CR) method [34] expressed as follows:

$$\ln\left[\frac{g(\alpha)}{T^2}\right] = \ln\left[\frac{A.R}{\beta.E}\right] - \frac{E}{R.T} \tag{7}$$

By plotting $\ln[g(\alpha)/T^2]$ versus $1/T$, the apparent activation energy and the apparent pre-exponential factor may be obtained.

3 Results and discussion

3.1 Characterization of materials

The results of microalgae characterization were shown in Table 3. According to these results, it was seen that

Fig. 1 FTIR spectra of microalga and biochar

Table 4 ANOVA for the quadratic model

| Source	Sum of squares	Degree of freedom (df)	Mean square	F value	p value	Remark
Model	1789.2570	9	198.8063	66.71404	< 0.0001	Significant
X_1	1152.7200	1	1152.7200	386.8217	< 0.0001	Significant
X_2	22.61281	1	22.61281	7.588248	0.0283	Significant
X_3	91.3952	1	91.3952	30.66976	0.0009	Significant
X_1X_2	0.003025	1	0.003025	0.001015	0.9755	
X_1X_3	70.0569	1	70.0569	23.5092	0.0019	Significant
X_2X_3	7.2900	1	7.2900	2.446327	0.1618	
X_1^2	397.7424	1	397.7424	133.4716	< 0.0001	Significant
X_2^2	17.59561	1	17.59561	5.904612	0.0454	Significant
X_3^2	9.622687	1	9.622687	3.229113	0.1154	
Residual	20.85985	7	2.979978			
Lack of fit	20.83013	3	6.943375	934.5054	< 0.0001	Significant
Pure error	0.02972	4	0.00743			
Cor total	1810.1170	16				

$R^2 = 0.988$; adjusted-$R^2 = 0.973$; predicted-$R^2 = 0.815$; Adeq precision = 25.420

C. vulgaris has high carbohydrate, lipid, and protein contents. Therefore, it can be used for different areas such as biodiesel, biogas, and animal feed production [35]. The moisture and ash content of *C. vulgaris* were found as 6.78 and 4.90%, respectively. In the literature, the moisture content of *Chlorella* sp. was reported as 9.1 and 5.39% by Agrawal and Chakraborty [20] and Miao et al. [16], respectively. The ash content of *Chlorella* sp. was also reported as 6.36% by Miao et al. [16] and 5.71% by Kent et al. [36]. Besides, the microalga has high volatile matter content because of high lipid, protein, and carbohydrate contents.

The FTIR spectrums of raw material and biochar were shown in Fig. 1. The spectrum of raw microalga showed seven characteristic signals at 3273, 2920, 1629, 1535, 1259, 1031, and 748 cm^{-1}. The peak at 3273 cm^{-1} can be in charge of the humidity [37, 38]. The absorption bands at 2920 and 1535 cm^{-1} were characteristic of the C–H stretching vibration and C=C stretching vibration, respectively. The peaks at 1629

and 1259 cm^{-1} were due to the protein content [39]. The peak at 1031 cm^{-1} was due to the carbohydrates content [40].

When the FTIR spectrum of biochar was compared with the spectrum of raw material, it was seen that significant changes occurred because of the high temperature in the pyrolysis process. The high temperature generated a decrease in several peaks such as at 3273 cm^{-1} (O–H stretching) and 2920 cm^{-1} (C–H stretching). Liu et al. [41] reported that the reasons for this are the change of chemical bonds and the gasification of some volatiles with increasing temperature. Major et al. [42] also reported that the high temperature in the pyrolysis process causes the transition from aliphatic to aromatic structure, aromatic ring formation, and H deformation. The peak at 760 cm^{-1} indicated pyridine in biochar which one of the nitrogen compounds is generally observed during pyrolysis [43]. The peaks between 1300 and 1000 cm^{-1} (-O-C-O stretching) were attributed to the transformation products of cellulose component of algal biomass [44].
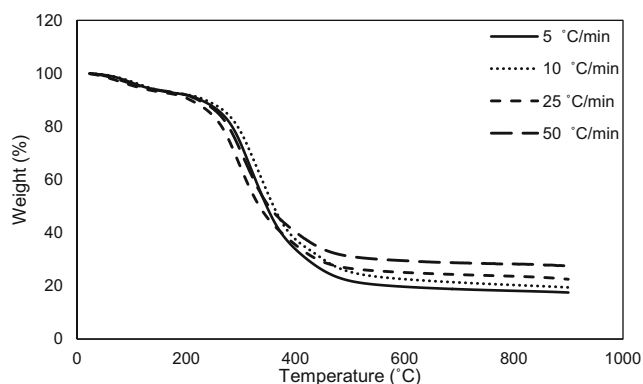
3.2 Statistical analysis of biochar production process

The experimental results were given in Table 1 and the relationship between biochar yield and the three process parameters was fitted to a quadratic model. This model for biochar production in terms of coded factors was represented as Eq. (8):

$$Y_{\text{Biocharyield}} = 20.59 - 12X_1 + 1.68X_2 - 3.38X_3$$
$$+ 0.03X_1X_2 + 4.19X_1X_3 + 1.35X_2X_3$$
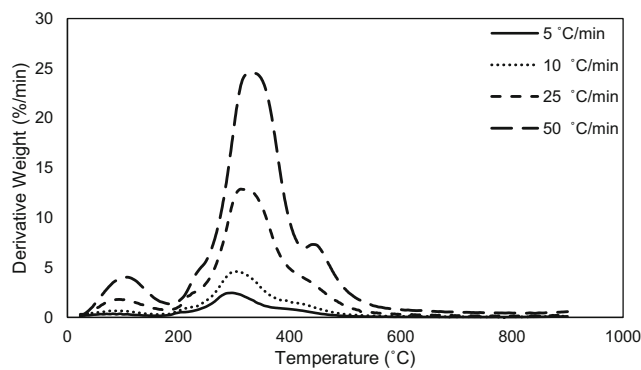$$+ 9.72X_1^2 + 2.04X_2^2 + 1.51X_3^2 \qquad (8)$$

Fig. 2 TG curves of *Chlorella vulgaris*

Fig. 3 DTG curves of *Chlorella vulgaris*

Fig. 4 Plots for activation energy calculation at various conversions by KAS method

The fitness of the model was tested by using analysis of variance (ANOVA), and ANOVA data were listed in Table 4. It can be seen in Table 4 that the model F value of 66.71 implied that the model is significant. If the p value is less than 0.05, it indicated that model terms are significant. In this study, $X_1, X_2, X_3, X_1X_3, X_1{}^2, X_2{}^2$ are significant model terms. F value for lack of fit of 934.51 implied that it is significant. Adeq precision value of 25.420 indicates an adequate signal.

The R^2, adjusted-R^2, and predicted-R^2 values were determined as 0.988, 0.973, and 0.815, respectively. As the value of R^2 approaches 1, it substantiated a better correlation between observed and predicted values [45]. So, the R^2 value represented that only about 2% of the total variation was not explained by the respective model.

As shown in Eq. (8) and Table 4, the selected parameters were all significant factors for biochar production from microalgal biomass. Temperature, the largest coefficient in the Eq. (8), and retention time have negative effects; on the contrary, heating rate has a positive effect on the yield of the solid product. According to the studies of Thangalazhy-Gopakumar et al. [46] and Li et al. [47], the primary degradation of biomass occurs in low carbonization temperatures. An increase in temperature causes the conversion of volatile products to lower molecular organic components and gas products. And more volatile products occur with the increasing temperature. Katyal et al. [48] reported that the effect of heating rate on char yield was seen clearly at low carbonization temperatures (< 400 °C); on the other
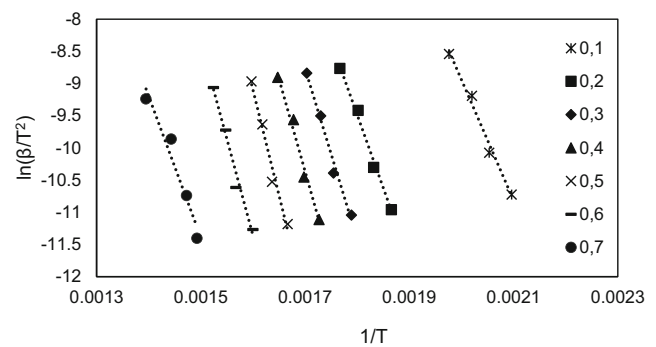
hand, this effect was not observed much at high carbonization temperatures (> 700 °C). It can be seen that the effect of these parameters on biochar yield is compatible with the result of studies that were performed with different biomass resources such as wood [49], pine dust [50], grass [51], soybean and peanut shell [52], olive stone [53], and algae [54] in the literature.

3.3 Thermogravimetric analysis of *Chlorella vulgaris*

TG and DTG curves of *Chlorella vulgaris* were shown in Figs. 2 and 3, respectively. According to these curves, it was seen that the degradation of *Chlorella vulgaris* was found in two different temperature regions, and Table 5 displays the temperature intervals and weight losses for these regions at the corresponding heating rates deduced from Figs. 2 and 3.

The first region at 30–180 °C for all heating rates resulted from the release of moisture content, and was also reported by Agrawal and Chakraborty [20]. The corresponding weight losses during the first stage were 7.2–7.38% for all heating rates. Most of the mass losses took place in the second regions. In the second region, there are 73.02, 70.15, 68.29, and 63.08% mass losses for the heating rate of 5, 10, 25, and 50 °C/min, respectively. According to the studies of Agrawal and Chakraborty [20] and Peng et al. [55], the reason for these mass losses was the degradation of organic materials such as carbohydrate, lipid, and protein. It can be seen in Table 5 that there is an increase in the initial and final temperatures of various stages with an increase in the heating rate.

Table 5 Temperature intervals for different regions

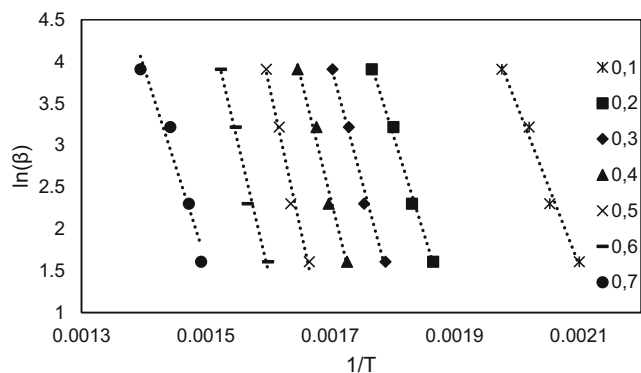| Heating rate (°C/min)	First region		Second region		Residue
	Temperature intervals (°C)	Weight loss (%)	Temperature intervals (°C)	Weight loss (%)	
5	30–170	7.38	170–541	73.02	17.49
10	30–180	7.32	180–548	70.15	19.44
25	30–183	7.23	183–557	68.29	22.46
50	30–187	7.20	187–575	63.08	27.46

Fig. 5 Plots for activation energy calculation at various conversions by FWO method

The maximum value of the decomposition rate increased with heating rate as can be observed from Fig. 3.

3.4 Pyrolysis kinetics

The KAS, FWO, and Coats-Redfern methods were used to evaluate the kinetic parameters for *Chlorella vulgaris*. Figures 4 and 5 showed non-isothermal plots of KAS method and FWO method at heating rates of 5, 10, 25, and 50 °C/min for conversions ranging from 0.1 to 0.7 to determine the activation energy. The activation energies and regression coefficients calculated by the KAS and FWO methods were shown in Table 6.

It can be seen in Table 6 that the regression coefficients were between 0.95 and 1 for all correlated lines shown in Figs. 4 and 5. The results indicated that these methods were suitable for evaluating the pyrolysis of *Chlorella vulgaris*. The activation energy values calculated from KAS and FWO methods were in good agreement except with a difference of ±3 in the value. The average activation energy values were calculated as 214.80 and 213.57 kJ/mol for KAS and FWO methods, respectively. When compared with other studies in the literature, it was seen that there were different activation energy values. Chen et al. [56] found that the average activation energy values of pyrolysis of *Chlorella vulgaris* calculated by KAS and FWO were 335.69 and 329.51 kJ/mol, respectively. Agrawal and Chakraborty [20] also reported that the average activation energy values calculated by KAS and FWO were 66.7 and 61.7 kJ/mol, respectively.

It can be seen in Table 6 that the increase in the degree of conversion from initial to 50% was accompanied by an increase in the activation energy. Radhakumari et al. [18] reported that the reason for this increase was the high energy requirement for degradation of microalga constituents such as hemicellulose and cellulose. Then, a decrease in activation energy was observed for the increase in the degree of conversion from 50 to 70% for both KAS and FWO methods. The same behavior was observed also at the other studies in the literature such as Radhakumari et al. [18] and Plis et al. [57]. Radhakumari et al. [18] reported that the activation energy calculated by KAS and FWO methods increased with the increase of conversion from initial to 0.3 and then it decreased with the increase of conversion from 0.3 to 0.7.

The kinetic parameters calculated by the Coats-Redfern method were also presented in Table 7. It can be seen in Table 7 that the activation energy values of pyrolysis of *Chlorella vulgaris* varied from 13.29 to 52.66 kJ/mol at heating rates of 5, 10, 25, and 50 °C/min for various models. For all heating rates, the D_3 model had the highest activation energy values in all models. These values were found as 45.33, 46.63, 52.66, and 51.72 kJ/mol at heating rates of 5, 10, 25, and 50 °C/min, respectively. When the regression coefficients were examined, it was seen that R_1, R_2, and R_3 kinetic models had relatively lower regression coefficients values than the other models for all heating rates. The most suitable kinetic model was found as F_3 for heating rates of 5 and 10 °C/min, F_2 for a heating rate of 25 °C/min, and D_3 for a heating rate of 50 °C/min.

4 Conclusion

Chlorella vulgaris is one of the most cultivated microalgae species in the world because of being used in many different areas such as energy production and pharmaceutical industry. In this study, *Chlorella vulgaris* was used for biochar production and the effects of process conditions on biochar yield were investigated statistically using Box-Behnken experimental design. Furthermore, the kinetics and mechanism of pyrolysis of *Chlorella vulgaris* were evaluated from the thermogravimetric data using KAS, FWO, and CR methods. Based on

Table 6 Activation energy (E) values calculated by KAS and FWO methods

Conversion (α)	KAS		FWO	
	E (kJ/mol)	R^2	E (kJ/mol)	R^2
0.1	150.51	0.984	150.88	0.985
0.2	189.63	0.991	189.03	0.992
0.3	220.59	0.984	218.82	0.985
0.4	238.77	0.980	236.42	0.982
0.5	272.97	0.976	269.26	0.978
0.6	249.43	0.975	247.31	0.977
0.7	181.73	0.950	183.78	0.955
Average	214.80		213.57	

Table 7 Kinetics parameters obtained by Coats-Redfern (CR) method

$g(\alpha)$	5 °C/min		10 °C/min		25 °C/min		50 °C/min	
	E (kJ/mol)	R^2	E (kJ/mol)	R^2	E (kJ/mol)	R^2	E (kJ/mol)	R^2
D_1	36.39	0.909	38.63	0.924	42.58	0.940	42.65	0.944
D_2	40.46	0.926	42.32	0.936	47.13	0.950	46.80	0.951
D_3	45.33	0.943	46.63	0.947	52.66	0.960	51.72	0.956
D_4	42.07	0.932	43.75	0.940	48.96	0.954	48.43	0.953
R_1	13.29	0.829	14.41	0.860	16.39	0.897	16.42	0.906
R_2	16.56	0.887	17.34	0.901	20.06	0.930	19.74	0.929
R_3	17.76	0.902	18.41	0.912	21.42	0.938	20.95	0.935
F_1	20.32	0.927	20.66	0.930	24.36	0.950	23.54	0.943
F_2	29.38	0.967	28.43	0.960	34.82	0.963	32.62	0.950
F_3	40.27	0.977	37.63	0.969	47.51	0.956	43.47	0.942

the results presented in this paper, the following conclusions were found:

- The maximum biochar yield was found as 53.61% at the temperature of 300 °C, the heating rate of 15 °C/min, and the retention time of 0 min. The minimum biochar yield was also found as 18.41% at the temperature of 700 °C, the heating rate of 15 °C/min, and the retention time of 30 min.
- According to the obtained statistical results, the temperature was the most effective parameter among the examined parameters. Although the yield of biochar decreased with increasing temperature and retention time, the yield increased with increasing heating rate. The obtained R^2, adjusted-R^2, and predicted-R^2 values were determined as 0.9885, 0.9737, and 0.8159, respectively, and this means a better correlation between the observed and predicted values.
- The average activation energy values were calculated as 214.80 and 213.57 kJ/mol for KAS and FWO methods, respectively. Since the regression coefficients were between 0.95 and 1, it can be said that KAS and FWO methods are suitable for evaluating the pyrolysis of *Chlorella vulgaris*.
- The activation energy values calculated by the CR method varied from 13.29 to 52.66 kJ/mol at the heating rates of 5, 10, 25, and 50 °C/min for various models.
- According to the regression coefficients calculated by CR method, the most suitable kinetic model was found as F_3 for heating rates of 5 and 10 °C/min, F_2 for a heating rate of 25 °C/min, and D_3 for a heating rate of 50 °C/min.
- The kinetic expressions and statistical results obtained in the present work can be used for future studies to model the process and optimize biochar yield from pyrolysis of microalgae and design various pyrolysis systems.

References

1. Dincer I, Rosen MA (1999) Energy, environment and sustainable development. Appl Energy 64(1–4):427–440
2. Adelard L, Poulsen TG, Rakotoniaina V (2015) Biogas and methane yield in response to co-and separate digestion of biomass wastes. Waste Manage Res 33(1):55–62
3. Özçimen D (2013) An approach to the characterization of biochar and bio-oil. Renew Energy Sustain Future iConcept Press:41–58
4. Demirbaş A (2001) Biomass resource facilities and biomass conversion processing for fuels and chemicals. Energy Convers Manag 42(11):1357–1378
5. Bach Q-V, Chen W-H (2017) A comprehensive study on pyrolysis kinetics of microalgal biomass. Energy Convers Manag 131:109–116
6. Alam F, Mobin S, Chowdhury H (2015) Third generation biofuel from algae. Proced Eng 105:763–768
7. Özçimen D, İnan B, Koçer AT, Reyimu Z (2016) Sustainable biorefinery design for algal biofuel production. In: Biofuels: production and future perspectives. CRC Press, pp 431–460
8. Nautiyal P, Subramanian K, Dastidar M (2014) Production and characterization of biodiesel from algae. Fuel Process Technol 120:79–88
9. Bohutskyi P, Ketter B, Chow S, Adams KJ, Betenbaugh MJ, Allnutt FT, Bouwer EJ (2015) Anaerobic digestion of lipid-extracted *Auxenochlorella protothecoides* biomass for methane generation and nutrient recovery. Bioresour Technol 183:229–239
10. Reyimu Z, Özçimen D (2017) Batch cultivation of marine microalgae *Nannochloropsis oculata* and *Tetraselmis suecica* in treated municipal wastewater toward bioethanol production. J Clean Prod 150:40–46
11. Chaiwong K, Kiatsiriroat T, Vorayos N, Thararax C (2013) Study of bio-oil and bio-char production from algae by slow pyrolysis. Biomass Bioenergy 56:600–606

12. Kim Y-M, Lee HW, Kim S, Watanabe C, Park Y-K (2015) Non-isothermal pyrolysis of citrus unshiu peel. Bioenergy Res 8(1):431–439

13. Özyurtkan MH, Özçimen D, Meriçboyu AE (2008) Investigation of the carbonization behavior of hybrid poplar. Fuel Process Technol 89(9):858–863

14. Bird MI, Wurster CM, de Paula Silva PH, Bass AM, De Nys R (2011) Algal biochar—production and properties. Bioresour Technol 102(2):1886–1891

15. Yanik J, Stahl R, Troeger N, Sinag A (2013) Pyrolysis of algal biomass. J Anal Appl Pyrolysis 103:134–141

16. Miao X, Wu Q, Yang C (2004) Fast pyrolysis of microalgae to produce renewable fuels. J Anal Appl Pyrolysis 71(2):855–863

17. Yang X, Wang X, Zhao B, Li Y (2014) Simulation model of pyrolysis biofuel yield based on algal components and pyrolysis kinetics. Bioenergy Res 7(4):1293–1304

18. Radhakumari M, Prakash DJ, Satyavathi B (2016) Pyrolysis characteristics and kinetics of algal biomass using tga analysis based on ICTAC recommendations. Biomass Convers Biorefin 6(2):189–195

19. Plis A, Lasek J, Skawińska A, Zuwała J (2015) Thermochemical and kinetic analysis of the pyrolysis process in *Cladophora glomerata* algae. J Anal Appl Pyrolysis 115:166–174

20. Agrawal A, Chakraborty S (2013) A kinetic study of pyrolysis and combustion of microalgae *Chlorella vulgaris* using thermogravimetric analysis. Bioresour Technol 128:72–80

21. Tekindal MA, Bayrak H, Ozkaya B, Genç Y (2012) Box-Behnken experimental design in factorial experiments: the importance of bread for nutrition and health. Turk J Field Crops 17(2):115–123

22. Brassard P, Godbout S, Raghavan V, Palacios JH, Grenier M, Zegan D (2017) The production of engineered biochars in a vertical auger pyrolysis reactor for carbon sequestration. Energy 10(3):288

23. Koçer AT, Özçimen D (2018) Investigation of the biogas production potential from algal wastes. Waste Manag Res 36:1100–1105

24. Dubois M, Gilles KA, Hamilton JK, Rebers PT, Smith F (1956) Colorimetric method for determination of sugars and related substances. Anal Chem 28(3):350–356

25. Soxhlet F (1879) Die gewichtsaiialytische Bestimmung des Milchfettes; von. Polytechnology 232:461

26. Lowry OH, Rosebrough NJ, Farr AL, Randall RJ (1951) Protein measurement with the Folin phenol reagent. J Biol Chem 193(1):265–275

27. García R, Pizarro C, Lavín AG, Bueno JL (2013) Biomass proximate analysis using thermogravimetry. Bioresour Technol 139:1–4

28. Koçer AT, Mutlu B, Özçimen D (2016) Algal biochar production from macroalgal wastes. In: Eurasia 2016 Waste Management Symposium. pp 777–781

29. Keattch CJ (1969) An introduction to thermogravimetry. Heyden. Co-operation with Sadtler Research Laboratories, Philadelphia

30. Shih YF (2009) Thermal degradation and kinetic analysis of biodegradable PBS/multiwalled carbon nanotube nanocomposites. J Polym Sci B Polym Phys 47(13):1231–1239

31. Kissinger HE (1957) Reaction kinetics in differential thermal analysis. Anal Chem 29(11):1702–1706

32. Ozawa T (1965) A new method of analyzing thermogravimetric data. Bull Chem Soc Jpn 38(11):1881–1886

33. Flynn JH, Wall LA (1966) A quick, direct method for the determination of activation energy from thermogravimetric data. J Polym Sci Part B Polym Lett 4(5):323–328

34. Coats AW, Redfern J (1964) Kinetic parameters from thermogravimetric data. Nature 201(4914):68–69

35. Özçimen D, İnan B, Akış S, Koçer AT (2015) Utilization alternatives of algal wastes for solid algal products. In: Algal biorefineries. Springer, pp 393–418

36. Kent M, Welladsen HM, Mangott A, Li Y (2015) Nutritional evaluation of Australian microalgae as potential human health supplements. PLoS One 10(2):e0118985

37. Gibbons G, Goad L, Goodwin T (1968) The identification of 28-isofucosterol in the marine green algae *Enteromorpha intestinalis* and *Ulva lactuca*. Phytochem 7(6):983–988

38. Karbowiak T, Ferret E, Debeaufort F, Voilley A, Cayot P (2011) Investigation of water transfer across thin layer biopolymer films by infrared spectroscopy. J Membr Sci 370(1–2):82–90

39. Ponnuswamy I, Madhavan S, Shabudeen S (2013) Isolation and characterization of green microalgae for carbon sequestration, waste water treatment and bio-fuel production. Int J Bio-Sci Bio-Technol 5(2):17–25

40. Dilna SV, Surya H, Aswathy RG, Varsha KK, Sakthikumar DN, Pandey A, Nampoothiri KM (2015) Characterization of an exopolysaccharide with potential health-benefit properties from a probiotic *Lactobacillus plantarum* RJF4. LWT Food Sci Technol 64(2):1179–1186

41. Liu Y, He Z, Uchimiya M (2015) Comparison of biochar formation from various agricultural by-products using FTIR spectroscopy. Mod Appl Sci 9(4):246

42. Major J, Steiner C, Downie A, Lehmann J (2012) Biochar effects on nutrient leaching. In: Biochar for environmental management. Routledge, pp 303–320

43. Zhao S-X, Ta N, Wang X-D (2017) Effect of temperature on the structural and physicochemical properties of biochar with apple tree branches as feedstock material. Energy 10(9):1293

44. Apaydın-Varol E, Pütün AE (2012) Preparation and characterization of pyrolytic chars from different biomass samples. J Anal Appl Pyrolysis 98:29–36

45. Gülyurt MÖ, Özçimen D, Inan B (2016) Biodiesel production from *Chlorella protothecoides* oil by microwave-assisted transesterification. Int J Mol Sci 17 (4):579

46. Thangalazhy-Gopakumar S, Adhikari S, Ravindran H, Gupta RB, Fasina O, Tu M, Fernando SD (2010) Physiochemical properties of bio-oil produced at various temperatures from pine wood using an auger reactor. Bioresour Technol 101(21):8389–8395

47. Li W, Yang K, Peng J, Zhang L, Guo S, Xia H (2008) Effects of carbonization temperatures on characteristics of porosity in coconut shell chars and activated carbons derived from carbonized coconut shell chars. Ind Crop Prod 28(2):190–198

48. Katyal S, Thambimuthu K, Valix M (2003) Carbonisation of bagasse in a fixed bed reactor: influence of process variables on char yield and characteristics. Renew Energy 28(5):713–725

49. Titiladunayo IF, McDonald AG, Fapetu OP (2012) Effect of temperature on biochar product yield from selected lignocellulosic biomass in a pyrolysis process. Waste Biomass Valoriz 3(3):311–318

50. Anderson CR, Condron LM, Clough TJ, Fiers M, Stewart A, Hill RA, Sherlock RR (2011) Biochar induced soil microbial community change: implications for biogeochemical cycling of carbon, nitrogen and phosphorus. Pedobio 54(5–6):309–320

51. Kumar S, Masto RE, Ram LC, Sarkar P, George J, Selvi VA (2013) Biochar preparation from *Parthenium hysterophorus* and its potential use in soil application. Ecol Eng 55:67–72

52. Ahmad M, Lee SS, Dou X, Mohan D, Sung J-K, Yang JE, Ok YS (2012) Effects of pyrolysis temperature on soybean stover-and

peanut shell-derived biochar properties and TCE adsorption in water. Bioresour Technol 118:536–544

53. Karakaş C, Özçimen D, İnan B (2017) Potential use of olive stone biochar as a hydroponic growing medium. J Anal Appl Pyrolysis 125:17–23

54. Chaiwong K, Kiatsiriroat T, Vorayos N, Thararax C (2012) Biochar production from freshwater algae by slow pyrolysis. Maejo Int J Sci Technol 6(2):186

55. Peng W, Wu Q, Tu P (2001) Pyrolytic characteristics of heterotrophic *Chlorella protothecoides* for renewable bio-fuel production. J Appl Phycol 13(1):5–12

56. Chen C, Ma X, He Y (2012) Co-pyrolysis characteristics of microalgae *Chlorella vulgaris* and coal through TGA. Bioresour Technol 117:264–273

57. Plis A, Lasek J, Skawińska A (2017) Kinetic analysis of the combustion process of *Nannochloropsis gaditana* microalgae based on thermogravimetric studies. J Anal Appl Pyrolysis 127:109–119